Check for updates

Covalently linked pyrene antennas for optically dense yet aggregation-resistant light-harvesting systems†

Lubna Salah, [ID][a] Saad Makhseed, [ID][a] Basma Ghazal, [ID][b] Ahmed Abdel Nazeer, [ID][c] Marc K. Etherington, [ID][d] Carlito S. Ponseca Jr., [ID][e] Chunyong Li, [ID][f] Andrew P. Monkman, [ID][f] Andrew Danos [ID]*[f] and Ali Shuaib [ID]*[g]

In this study we present a novel energy transfer material inspired by natural light-harvesting antenna arrays, zinc(II) phthalocyanine-pyrene (**ZnPcPy**). The **ZnPcPy** system facilitates energy transfer from 16 covalently linked pyrene (Py) donor chromophores to the emissive central zinc(II) phthalocyanine (ZnPc) core. Nearly 98% energy transfer efficiency is determined from the changes in emission decay rates between free **MePy** to covalently linked Py, supported by comparisons of photoluminescence quantum yields using different excitation wavelengths. A comparative analysis of **ZnPcPy** and an equivalent mixture of **ZnPc** and **MePy** demonstrates the superior light-harvesting performance of the covalently linked system, with energy transfer rates 9705 times higher in the covalently bound system. This covalent strategy allows for very high loadings of absorbing Py chromophores to be achieved while also avoiding exciton quenching that would otherwise arise, with the same strategy widely applicable to other pairs of Főrster resonance energy transfer (FRET) chromophores.

Introduction

Molecular light-harvesting is arguably the most important physicochemical process supporting life on Earth.[1,2] With rare exceptions (*e.g.*, geothermal and nuclear energy),[3] almost all our energy is derived directly or indirectly from the absorption of sunlight.[4] While inorganic light-harvesting technologies such as silicon photovoltaics have advanced significantly during the past 50 years, its sophistication and scale is still miniscule compared to the equivalent evolved molecular

[a] *Department of Chemistry, Faculty of Science, Kuwait University, P. O. Box 5969, Safat 13060, Kuwait*

[b] *Organometallic and Organometalloid Chemistry Department, National Research Centre, Giza, Egypt*

[c] *Organometallic and Organometalloid Department, National Research Centre, Dokki, Cairo, 12622, Egypt*

[d] *Department of Mathematics, Physics & Electrical Engineering, Northumbria University, Ellison Place, Newcastle upon Tyne, NE1 8ST, UK*

[e] *Mathematics and Natural Science Department, Gulf University for Science and Technology, Kuwait*

[f] *Department of Physics, Durham University, South Road, Durham, DH1 3LE, UK. E-mail: andrew.danos@durham.ac.uk*

[g] *Biomedical Engineering Unit, Department of Physiology, Faculty of Medicine, Kuwait University, P. O. Box 24923, Safat 13110, Kuwait. E-mail: ali.shuaib@ku.edu.kw*

† Electronic supplementary information (ESI) available. See DOI: https://doi.org/10.1039/d3cp02586a

process: photosynthesis.[5,6] In photosynthesis, the light-harvesting complex features many light-absorbing pigments, which transfer absorbed energy to the central reaction center to drive the endothermic fixation of atmospheric carbon dioxide.[7] Mirroring this approach, the well-developed field of photocatalysis also uses light absorption to activate a wide range of otherwise inaccessible chemistry.[8–10]

Improving the performance and feasibility of photocatalysts often requires increasing their absorption cross-section,[11] allowing higher reaction turnover with smaller amounts of catalyst or more complete absorption of a fixed quantity of illumination.[12] However, it is often challenging to engineer altered absorption bands without also impacting the photocatalytic reaction pathway.[13] Once again taking inspiration from photosynthesis,[14] it is instead possible to develop separate absorbing pigments which activate a non-absorbing reaction centre by Főrster resonance energy transfer (FRET).[15] In this way the separate parts of the overall photocatalysis system can be better specialized to their specific roles. Similar specialisation and energy transfer between components is also employed to achieve high performance in hyperfluorescent OLEDs[16–20] and in triplet–triplet annihilation upconversion systems.[21,22]

While the photosynthesis light-harvesting complex is exquisitely optimsed by millions of years of evolution, equivalent synthetic light-harvesting platforms are not as advanced.[23–25]

Typically, the FRET acceptor and the FRET donor are simply mixed together, either in solution or immobilized in (or along) a polymer host.[26,27] Often this approach puts limitations on the types and concentrations of light-absorbers to be used though, as aggregation of these can lead to unwanted non-radiative decay that competes with emission and/or FRET.[28–30] For example, small aromatic hydrocarbons such as perylene or pyrene (Py) possess strong absorption bands, making them appealing for use as molecular absorbers. However, their flat and electron-rich structure also makes them highly susceptible to aggregation, with many studies reporting chemical modifications or other strategies designed to prevent this.[31,32]

In previous work we have successfully synthesised **ZnPcPy**.[33] Here we consider the optical and energy transfer properties of this material, taking inspiration from the photosynthetic antenna array. In that biological system, aggregation is avoided with the absorbing dyes covalently fixed to the FRET acceptor, and unable to diffuse freely to form aggregate states.[34] Similarly here, without modification of the Py absorbing unit, **ZnPcPy** exhibits strong Py absorption with efficient zinc(II)-phthalocyanine (**ZnPc**) emission in solution, significantly outperforming two-component mixtures at equivalent concentrations, and able to access chromophore concentrations that would be otherwise detrimental to the unbound Py unit.

Results & discussion

Synthesis

The synthesis of zinc(II) phthalocyanine-pyrene (**ZnPcPy**) was carried out using alkyne-azide click chemistry, as previously reported in a published paper[33] and depicted in ESI,† Scheme S1. The structure of **ZnPcPy** was confirmed, as reported in the previous published study,[33] by several spectroscopic techniques including nuclear magnetic resonance (NMR), Fourier transform infrared (FT-IR), and MALDI-TOF, as well as CHN elemental analysis.[33] The molecular structures of zinc(II) phthalocyanine (**ZnPc**), methylpyrene (**MePy**), and **ZnPcPy** are illustrated in Fig. 1.

Optical properties

We first investigated the steady-state absorption and emission properties of **ZnPcPy**, its separate analogous components (**ZnPc** and **MePy**), and equivalent mixtures of those components in

Fig. 1 Structures of **ZnPc**, **MePy**, and **ZnPcPy**. The specific conformation of **ZnPcPy** shown is for illustrative purposes only.

dilute THF solution. Fig. 2(A) shows the typical B-band for **ZnPc** at 345 nm and the Q-band at 667 nm. The main Q-band redshifted to 687 nm in **ZnPcPy**, possibly due to the extended conjugation system associated with the appended Py units[35] (either through-bond or through-space), or by effective solvation of the ZnPc core by the surrounding Py units. The B-band of **ZnPcPy** was not resolvable underneath the strong absorption bands of the covalently bound Py units, which retained the same spectral shape as those of the unbound **MePy**.[36] Considering that each **ZnPcPy** molecule contains 16 bound Py subunits, it is surprising that the absorbance intensity of the 2 μM **ZnPcPy** solution does not match more closely that of an equivalent mixture of 2 μM **ZnPc** and 32 μM **MePy**. This could indicate some transfer of oscillator strength when Py is incorporated into the **ZnPc** electronic system, although the extinction coefficient remains very high overall: 4.76×10^5 M^{-1} cm^{-1} at 345 nm, compared to 4.28×10^4 M^{-1} cm^{-1} for **MePy**.

Comparing the overlapping positions of the **MePy** emission (Fig. 2(B), 350–400 nm, and Fig. S5, ESI†) with the **ZnPc** B-band absorption indicates the potential for FRET between the two subcomponents in the joined **ZnPcPy** compound. Indeed, qualitative evidence for this FRET is evident in the emission spectra of **ZnPcPy**, which when excited in the Py absorption band (345 nm) emits nearly exclusively from the **Pc** core (negligible Py emission, Fig. S3, ESI†). The identity of this **ZnPc** emission is confirmed by comparing with the emission spectra from both **ZnPcPy** and **ZnPc** when these are excited directly into their Q-band (∼615 nm), yielding emission only at ∼700 nm. In strong contrast, when a mixture of **ZnPc** and **MePy** is excited at 345 nm, simultaneous emission from both separate materials is observed. This immediately demonstrates the superior FRET rate in **ZnPcPy**, which is able to outcompete and quench the radiative emission of **MePy**.

To further develop upon the qualitative insights from the steady-state spectra and intensities, the photoluminescence quantum yields (PLQYs) and emission decay lifetimes of the solutions were also measured. As summarised in Table 1, for **MePy** excited at 345 nm we observe a PLQY of 6.5% and an emission decay lifetime of 17.3 ns. For **ZnPc**, the excited-state behaviour is very similar regardless of whether excitation occurs at 345 nm or 615 nm, with PLQYs of 25/25% and lifetimes of 3.6/3.5 ns, respectively. This indicates fast and efficient internal conversion from the higher excited states in **ZnPc** (which can be excited using 345 nm) down to the lowest singlet state, with no significantly active loss pathways interrupting transfer to S$_1$.

In **ZnPcPy** the optical properties are also strongly independent of the excitation wavelength. The PLQYs derived using 345 nm or 615 nm excitation are 16 and 18%, respectively, with only a vanishingly small contribution from the ∼400 nm Py band (Fig. S3, ESI†). The lifetime of the ∼700 nm emission band is also very similar to that of **ZnPc** and approximately invariant with the choice of excitation wavelength (3.2 and 3.1 ns at 345 and 615 nm excitation, respectively, decays and fits shown in Fig. S8–S11, ESI†). As in **ZnPc**, this invariance of both the emission lifetime and PLQY also indicates a very fast
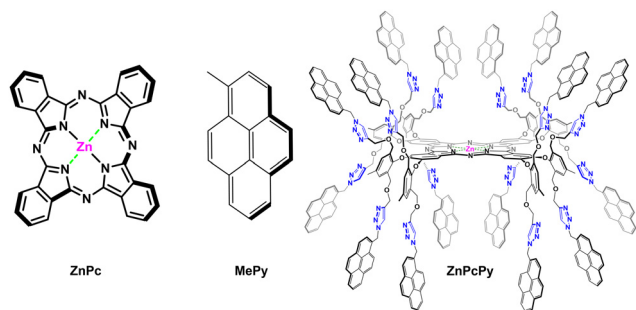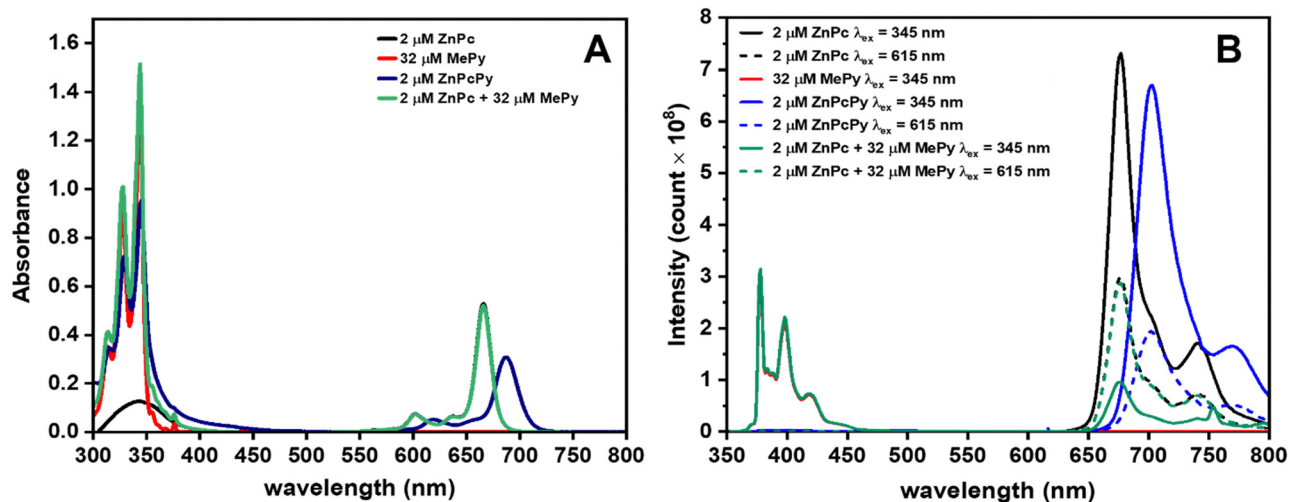
This journal is © the Owner Societies 2023

Phys. Chem. Chem. Phys., 2023, **25**, 24878–24882 | **24879**

Fig. 2 The absorption and emission properties for different compounds in THF. (A) Absorption spectra were acquired for 2 μM **ZnPc**, 32 μM **MePy**, 2 μM **ZnPcPy**, and a mixture containing 2 μM **ZnPc** and 32 μM **MePy**. (B) Emission spectra were recorded for the same samples, excited at either 345 or 615 nm.

Table 1 Optical properties of 2 μM **ZnPc**, 2 μM **MePy**, 2 μM **ZnPcPy**, and the mixture of 2 μM **ZnPc** + 32 μM **MePy** in THF solution

Parameter	2 μM **ZnPc**	2 μM **MePy**	2 μM **ZnPcPy**	Mixture of 2 μM **ZnPc** + 32 μM **MePy**
λ_{abs} (nm)	345, 667	310, 330, 345	314, 330, 345, 687	314, 327, 344, 667
λ_F (nm)	677	369, 376	696	377, 398, 678
ε (M^{-1} cm^{-1}) (log ε) 345 nm/667 or 687 nm	63 500 (4.80)/264 000 (5.42)	43 438 (4.64)/—	476 000 (5.68)/154 500 (5.19)	42 781 (4.63)/260 000 (5.41)
τ (ns) λ_{em} = 400 nm λ_{ex} = 345 nm	—	17.3	0.3	17.2
τ (ns) λ_{em} = 700 nm λ_{ex} = 345/615 nm	3.6/3.5	—/—	3.2/3.1	3.7/3.6
PLQY λ_{em} = 400 nm λ_{ex} = 345/615 nm	—/—	0.065/—	0.0002/—	0.053/—
PLQY λ_{em} = 700 nm λ_{ex} = 345/615 nm	0.25/0.25	—/—	0.16/0.18	0.043/0.24

and efficient transfer of excitation from higher excited states-including the Py groups-down to the ZnPc-centred S_1 state by both internal conversion and intramolecular FRET. In the presence of a hypothetical competing loss pathways, we would not expect that exciting the Py groups (345 nm excitation) would be able to give the same overall PLQY as exciting the ZnPc core directly (with 615 nm, which avoids any losses as excitons transfer from Py to ZnPc). Indeed, by comparing the lifetimes of the 400 nm Py emission in **MePy** (17.3 ns) and in **ZnPcPy** (0.3 ns), we can attribute the increased decay rate to FRET and estimate an energy transfer rate of 3.3×10^9 s^{-1}. This rate of excitation transfer is significantly faster than the radiative and nonradiative decay rates for **MePy** (3.8×10^6 and 5.4×10^7 s^{-1}, respectively), which explains how the **ZnPcPy** compound can avoid losses associated with the low PLQY of **MePy** emission, even when this group is predominantly excited (with 345 nm).

Based on the ratio of decay rates in **MePy**, this corresponds to a FRET efficiency of ~98%, which is also consistent with the unchanged PLQYs in **ZnPcPy** regardless of the excitation wavelength.

Compared with **ZnPcPy**, the energy transfer properties of an equivalent concentration mixture of **ZnPc** and **MePy** are considerably inferior. When excited using 345 nm light, the PLQY of both the **MePy** and **ZnPc** emission bands were very low (5.3 and 4.3% respectively), indicating some emission directly from the low-efficiency **MePy** and poor FRET transfer to the **ZnPc**. On the contrary, when the same **ZnPc** in the mixture was excited directly using 615 nm, the PLQY was largely unaffected by the presence of **MePy** (24%). Additionally, the emission lifetime of **MePy** hardly changed in the presence of **ZnPc**, decreasing from 17.3 to 17.2 ns, which corresponds to a FRET rate of only 3.4×10^5 s^{-1} and a FRET efficiency of 0.6%. Considering again the

24880 | Phys. Chem. Chem. Phys., 2023, 25, 24878–24882

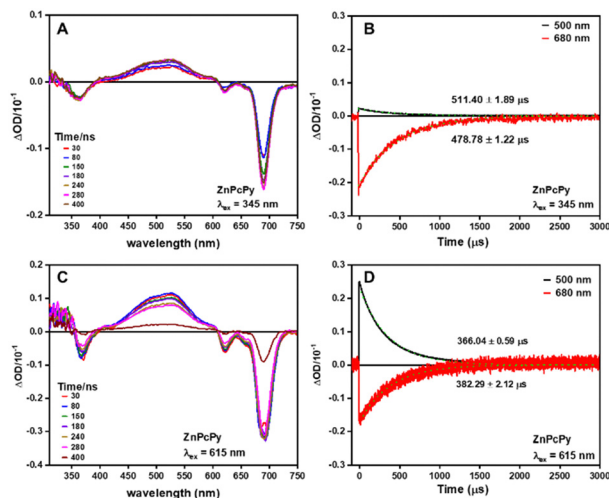This journal is © the Owner Societies 2023

Fig. 3 Transient absorption spectra (left) and decay traces (right) of **ZnPcPy** in THF when excited at (A), (B) 345 nm and (C), (D) 615 nm, respectively.

radiative and non-radiative decay rates of **MePy** (3.8×10^6 and 5.4×10^7 s^{-1}, respectively), it is clear that nearly all photons absorbed by untethered **MePy** are wasted. To achieve the same FRET rate as **ZnPcPy**, the mixture would require a concentration of **ZnPc** 9705 times higher; *i.e.* 32 μM of **MePy** with 17 mM of **ZnPc**. This extreme ratio of **ZnPc** would itself defeat the design strategy and purpose of a molecular antenna array, in which many absorbers are intended to funnel energy to a less concentrated emission or reaction centre.

Transient absorption spectra and kinetics were also investigated to gain insights into the internal energy transfer in **ZnPcPy** upon excitation at 345 nm and 615 nm (Fig. 3). The results demonstrate that the excited-state absorption spectra of **ZnPcPy** remain unchanged when excited at either of these wavelengths, suggesting that no additional decay pathways compete with the FRET process from Py to ZnPc groups. If alternative decay pathways were present, one would anticipate detecting an additional band in the excited-state absorption spectrum corresponding to a quenching state when excited at 345 nm but absent when excited at 615 nm. Furthermore, there is no indication of excited state absorptions or ground state bleaches from the Py chromophore (**MePy** measured separately, Fig. S7, ESI†), indicating FRET on a more rapid timescale than the measurement. We note that due to different ground state absorption intensities and pump beam photon fluxes, we do not attribute any meaning to the different intensities of the transient absorption spectra using the different excitation wavelengths.

The enhanced FRET efficiency observed in **ZnPcPy** can be primarily attributed to the covalent attachment of Py groups to the ZnPc core, which ensures consistent close proximity between chromophores. Given the strong dependence of FRET rate on distance, this short distance between chromophores can overcome the apparently small FRET spectral overlap. In contrast, the simple mixture of **ZnPc** and **MePy** experiences larger and more dynamic inter-chromophore distances

controlled by molecular diffusion, leading to a lower FRET rate. Even with identical molar concentration of chromophores in both **ZnPcPy** and the simple mixture, the importance of structural rigidity and fixed distances in preventing stacking and aggregation should not be underestimated. The covalent tethering of Py groups to the ZnPc core additionally creates a stable and well-defined spatial arrangement, reducing the accessibility of conformations that lead to intramolecular Py aggregates and maintaining consistent chromophore distances. This covalently linked configuration also decreases the probability of Py aggregates forming between molecules, as the concentrations of other **ZnPcPy** molecules is 16 times lower than the equivalent concentration of Py molecules in the mixture, with correspondingly 16 times lower rate of aggregate-forming molecular collisions.

Conclusions

In conclusion, we have shown that covalently linked pyrene antennas offer a promising approach for developing efficient and aggregation-resistant light-harvesting systems. Inspired by nature's photosynthetic antenna arrays, **ZnPcPy** exhibits exceptional energy transfer efficiency that greatly surpasses simple mixtures. Covalent bonds between the chromophores ensure consistent distances necessary for energy transfer, while the rigidity and geometric constraints help to prevent aggregate formation. While pyrene itself is not optimized for solar energy absorption, this strategy can be widely applied to other pairs of FRET-enabled chromophores to target different absorption ranges, even when the FRET overlap is small. Overall, covalently linked FRET systems showcase the power of nature-inspired design principles for engineering advanced light-harvesting systems, paving the way for further innovation and applications in the areas of photocatalysis, emissive materials for OLEDs, and solar energy management in the form of upconversion.

Conflicts of interest

There are no conflicts to declare.

Acknowledgements

References

1 G. Schlau-Cohen, *Interface Focus*, 2015, **5**, 20140088.

This journal is © the Owner Societies 2023

Phys. Chem. Chem. Phys., 2023, **25**, 24878–24882 | **24881**

2 H. Shang, M. Li and X. Pan, *Plants*, 2023, **12**, 1173.

3 V. M. Friebe, *Hacking Photosynthesis, PhD thesis, Research and graduation internal*, Vrije Universiteit Amsterdam, 2017.

4 M. A. Moran and W. L. Miller, *Nat. Rev. Microbiol.*, 2007, **5**, 792–800.

5 O. Inganäs and V. Sundström, *Ambio*, 2016, **45**, 15–23.

6 B. C. Tashie-Lewis and S. G. Nnabuife, *Chem. Eng. J. Adv.*, 2021, **8**, 100172.

7 M. Ballottari, J. Girardon, L. Dall'Osto and R. Bassi, *Biochim. Biophys. Acta, Bioenerg.*, 2012, **1817**, 143–157.

8 T. J. Blackburn, S. M. Tyler and J. E. Pemberton, *Anal. Chem.*, 2022, **94**, 515–558.

9 L. L. Tinker, N. D. McDaniel and S. Bernhard, *J. Mater. Chem.*, 2009, **19**, 3328–3337.

10 V. Jain, R. K. Kashyap and P. P. Pillai, *Adv. Opt. Mater.*, 2022, **10**, 2200463.

11 Z. Zafar, S. Yi, J. Li, C. Li, Y. Zhu, A. Zada, W. Yao, Z. Liu and X. Yue, *Energy Environ. Mater.*, 2022, **5**, 68–114.

12 J. Ge, Y. Zhang and S.-J. Park, *Materials*, 2019, **12**, 1916.

13 Q. Van Le, V.-H. Nguyen, T. D. Nguyen, A. Sharma, G. Rahman and D. L. T. Nguyen, *Chem. Eng. Sci.*, 2021, **237**, 116547.

14 M. R. Wasielewski, *Acc. Chem. Res.*, 2009, **42**, 1910–1921.

15 G. A. Jones and D. S. Bradshaw, *Front. Phys.*, 2019, **7**, 100.

16 K. Stavrou, S. Suresh, D. Hall, A. Danos, N. Kukhta, A. Slawin, S. Warriner, D. Beljonne, Y. Olivier and A. Monkman, *Adv. Opt. Mater.*, 2022, **10**(17), 2200688.

17 D. Hall, K. Stavrou, E. Duda, A. Danos, S. Bagnich, S. Warriner, A. M. Slawin, D. Beljonne, A. Köhler and A. Monkman, *Mater. Horiz.*, 2022, **9**, 1068–1080.

18 K. Stavrou, A. Danos, T. Hama, T. Hatakeyama and A. Monkman, *ACS Appl. Mater. Interfaces*, 2021, **13**, 8643–8655.

19 N. Haase, A. Danos, C. Pflumm, P. Stachelek, W. Brütting and A. P. Monkman, *Mater. Horiz.*, 2021, **8**, 1805–1815.

20 L. Salah, M. K. Etherington, A. Shuaib, A. Danos, A. A. Nazeer, B. Ghazal, A. Prlj, A. T. Turley, A. Mallick and P. R. McGonigal, *J. Mater. Chem. C*, 2021, **9**, 189–198.

21 A. Danos, R. W. MacQueen, Y. Y. Cheng, M. Dvořák, T. A. Darwish, D. R. McCamey and T. W. Schmidt, *J. Phys. Chem. Lett.*, 2015, **6**, 3061–3066.

22 R. W. MacQueen, Y. Y. Cheng, A. N. Danos, K. Lips and T. W. Schmidt, *RSC Adv.*, 2014, **4**, 52749–52756.

23 B. Ghazal, D. E. Nevonen, L. Salah, A. Shuaib, V. N. Nemykin and S. Makhseed, *Dyes Pigm.*, 2023, 111361.

24 A. Pinnola, *J. Exp. Bot.*, 2019, **70**, 5527–5535.

25 X. Li, L. E. Sinks, B. Rybtchinski and M. R. Wasielewski, *J. Am. Chem. Soc.*, 2004, **126**, 10810–10811.

26 N. J. Davis, R. W. MacQueen, D. A. Roberts, A. Danos, S. Dehn, S. Perrier and T. W. Schmidt, *J. Mater. Chem. C*, 2016, **4**, 8270–8275.

27 B. Zhang, G. Lyu, E. A. Kelly and R. C. Evans, *Adv. Sci.*, 2022, 2201160.

28 A. Husain, A. Ganesan, L. Salah, P. Kubát, B. Ghazal and S. Makhseed, *ChemPlusChem*, 2022, **87**, e202200275.

29 V. Sundström and T. Gillbro, *J. Chem. Phys.*, 1985, **83**, 2733–2743.

30 J. S. Huff, P. H. Davis, A. Christy, D. L. Kellis, N. Kandadai, Z. S. Toa, G. D. Scholes, B. Yurke, W. B. Knowlton and R. D. Pensack, *J. Phys. Chem. Lett.*, 2019, **10**, 2386–2392.

31 E. Aksoy, A. Danos, C. Varlikli and A. P. Monkman, *Dyes Pigm.*, 2020, **183**, 108707.

32 E. Aksoy, A. Danos, C. Li, A. P. Monkman and C. Varlikli, *J. Phys. Chem. C*, 2021, **125**, 13041–13049.

33 A. Husain, A. Ganesan, M. Sebastian and S. Makhseed, *Dyes Pigm.*, 2021, **184**, 108787.

34 L. Bar Eyal, R. Ranjbar Choubeh, E. Cohen, I. Eisenberg, C. Tamburu, M. Dorogi, R. Ünnep, M.-S. Appavou, R. Nevo and U. Raviv, *Proc. Natl. Acad. Sci. U. S. A.*, 2017, **114**, 9481–9486.

35 J. Ohshita, Y. Hatanaka, S. Matsui, Y. Ooyama, Y. Harima and Y. Kunugi, *Appl. Organomet. Chem.*, 2010, **24**, 540–544.

36 G. B. Ray, I. Chakraborty and S. P. Moulik, *J. Colloid Interface Sci.*, 2006, **294**, 248–254.

24882 | *Phys. Chem. Chem. Phys.*, 2023, **25**, 24878–24882

This journal is © the Owner Societies 2023